

Space Vector Modulation Technique for Direct Torque Control of Induction Motors

R. Kavitha, S. Poovizhi, M. R. Akila

R. M. K College of Engineering and Technology, TamilNadu, India

ABSTRACT

The PWM principle is used to control the output voltage of the three-phase inverters. There are many possible PWM techniques proposed in literature. Among these the space-vector PWM (SVM) method is an advanced PWM method and is possibly the best among all the PWM techniques for variable-frequency drive applications. The classical SVPWM which is used in the direct torque control of induction motor has the possible dynamic locus of the stator flux, and its different variation depending on the VSI states chosen. This locus is divided into six different sectors. The switching frequency used in this classical DTC method is high which causes switching losses.

A novel SVPWM technique is introduced to reduce the switching losses. In this technique the stator flux locus is divided into eight sectors. This concept can be applied to all control methods. Performance of torque and speed is not varied with six sector module

Keywords: Induction Motor Drives, VSI, Torque Control

I. INTRODUCTION

The space vector PWM (SVM) method is an advanced, computation intensive PWM method and is possibly the best among all the PWM techniques for variable frequency drive applications. Because of its superior performance characteristics, it has been finding wide spread application in recent years.

The PWM methods discuss so far have only considered implementation on a half-bridge of a three-phase bridge inverter. If the load neutral is connected to the centre tap of the dc supply, all the three half-bridges operate independently, giving satisfactory PWM performance. With a machine load, the load neutral is normally isolated, which causes interaction among the phases. This interaction was not considered before in PWM discussions. The SVM method considers this interaction of the phases and optimizes the harmonic content of the three-phase isolated neutral load. To understand the SVM theory the concept of rotating space vector is important. For example, if the three phase sinusoidal and balanced voltages given by the equations are applied to a three-phase induction motor, using following equations,

it can be shown that the space vector \bar{V} with magnitude V_m rotates in a circular orbit at angular velocity ω where the direction of rotation depends on the phase sequence of the voltages.

$$\begin{aligned} V_a &= V_m \cos \omega t \\ V_b &= V_m \cos(\omega t - \frac{2\pi}{3}) \\ V_c &= V_m \cos(\omega t + \frac{2\pi}{3}) \end{aligned} \quad (1)$$

$$\begin{aligned} \bar{V} &= v_{qs}^s - jv_{ds}^s \\ &= \left(\frac{2}{3}v_{as} - \frac{1}{3}v_{bs} - \frac{1}{3}v_{cs} \right) - j \left(-\frac{\sqrt{3}}{2}v_{bs} + \frac{\sqrt{3}}{2}v_{cs} \right) \\ &= \frac{2}{3} \left[v_{as} + \left(-\frac{1}{2} + j\frac{\sqrt{3}}{2} \right) v_{bs} + \left(-\frac{1}{2} - j\frac{\sqrt{3}}{2} \right) v_{cs} \right] \\ &= \frac{2}{3} [v_{as} + av_{bs} + a^2v_{cs}] \end{aligned} \quad (2)$$

With the sinusoidal three phase command voltages, the composite PWM fabrication at the inverter output should be such that the average voltages follow these command voltages with a minimum amount of harmonic distortion.

A three phase bridge inverter as shown in figure has $2^3=8$ permissible switching states.

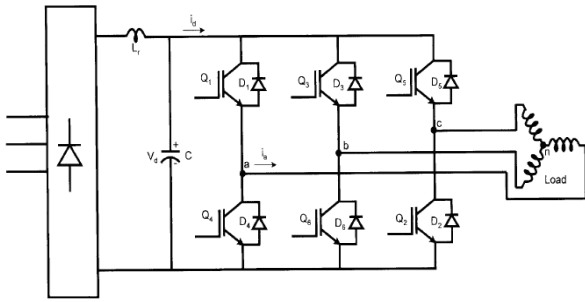


Figure 1 : Three Phase Bridge Inverter (shown with diode rectifier at front end)

The following table gives a summary of switching states and the corresponding phase-to-neutral voltages of an isolated neutral machine.

State	On devices	v_{an}	v_{bn}	v_{cn}	Space voltage vector
0	$Q_4 Q_6 Q_2$	0	0	0	$\bar{V}_0(000)$
1	$Q_1 Q_6 Q_2$	$2V_d/3$	$-V_d/3$	$-V_d/3$	$\bar{V}_1(100)$
2	$Q_1 Q_3 Q_2$	$V_d/3$	$V_d/3$	$-2V_d/3$	$\bar{V}_2(110)$
3	$Q_4 Q_3 Q_2$.	.	.	$\bar{V}_3(010)$
4	$Q_4 Q_3 Q_5$.	.	.	$\bar{V}_4(011)$
5	$Q_4 Q_6 Q_5$.	.	.	$\bar{V}_5(001)$
6	$Q_1 Q_6 Q_5$.	.	.	$\bar{V}_6(101)$
7	$Q_1 Q_3 Q_5$	0	0	0	$\bar{V}_7(111)$

Table 1 : Summary of Inverter Switching States

Consider, for example, state 1, when switches Q_1 , Q_6 and Q_2 are closed. In this state, phase 'a' is connected to the positive bus and phase 'b' and 'c' are connected to the negative bus. The simple circuit shown indicates that $V_{an}=2/3 V_d$, $V_{bn}= -1/3 V_d$, and $V_{cn}= -1/3 V_d$. The inverter has 6 active states (1-6) when voltage is impressed across the load, and two zero states (0 and 7) when the machine terminals are shorted through the lower devices or upper devices, respectively. The sets of phase voltages for each switching state can be combined with the help of equation (2.2) to derive the corresponding space vectors. The graphical derivation of $V_1(100)$ in figure (2) indicates that the vector has a magnitude of $2/3 V_d$ and is aligned in the horizontal direction as shown.

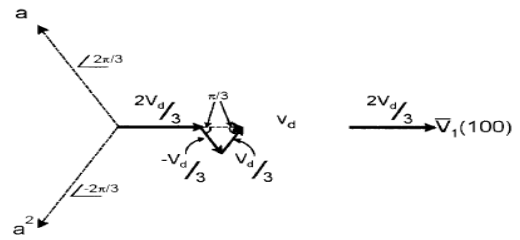


Figure 2 : Construction of Space Vector $V_1(100)$

In the same way all six active vectors and two zero vectors are divided and plotted.

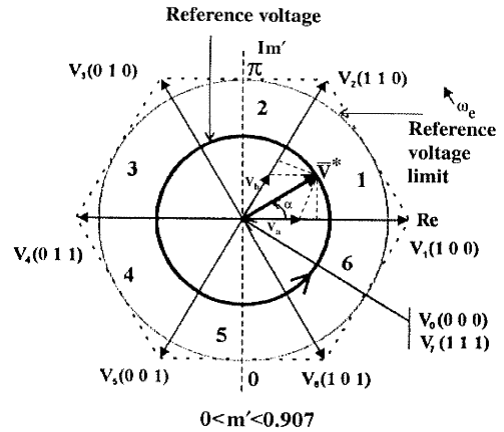


Figure 3 : Vector Diagram for Six Sectors

The active vectors are $\pi/3$ angle apart and describe a hexagon boundary (shown as dotted). The two zero vectors $V_0(000)$ and $V_7(111)$ are at origin.

The principal pulse width modulation (PWM) techniques are used in voltage fed inverters. The duty cycle modulated PWM principle was introduced earlier when discussing dc-dc converters. The inverter's fundamental voltage can be controlled and the harmonics can be attenuated (or eliminated) by creating selective notches in the square wave output. The square-wave inverter voltage control is possible by means of a thyristor rectifier located at the front end or a dc-dc converter at the input; output can be filtered by bulky passive filters. Phase-shift control of square-wave inverters also permits voltage control as well as lower order harmonics cancellation. However, electronic switching of voltage control as well as harmonic elimination is much more efficient and cost effective. However, this decreases the device switching frequency, which in turn decreases the switching loss.

B. Application Of Eight Sector SVPWM

1. Direct torque and flux control of induction motor

An advanced scalar control technique, known as direct torque and flux control (DTC) or direct self-control was introduced for voltage-fed PWM inverter drives, this technique was claimed to have nearly comparable performance with vector controlled drives. The scheme as the name indicates is the direct control of the torque and stator flux of a drive by inverter voltage space vector selection through a look up table.

2. Torque expression with stator and rotor fluxes

The torque expression given in equation,

$$T_e = \frac{3}{2} \left(\frac{P}{2} \right) (\psi_{ds}^s i_{qs}^s - \psi_{qs}^s i_{ds}^s) \quad (3)$$

Can be expressed as in the vector form as,

$$\bar{T}_e = \frac{3}{2} \left(\frac{P}{2} \right) \bar{\psi}_s \times \bar{I}_s \quad (4)$$

Where, $\bar{\psi}_s = \psi_{qs}^s - j \psi_{ds}^s$, $\bar{I}_s = i_{qs}^s - j i_{ds}^s$

In this equation \bar{I}_s is to be replaced by rotor flux $\bar{\psi}_r$. In the complex form, $\bar{\psi}_s$ and $\bar{\psi}_r$ can be expressed as functions of currents as

$$\begin{aligned} \bar{\psi}_s &= L_s \bar{I}_s + L_m \bar{I}_r \\ \bar{\psi}_r &= L_r \bar{I}_r + L_m \bar{I}_s \end{aligned} \quad (5)$$

Eliminating \bar{I}_r from the equation, we get

$$\bar{\psi}_s = \frac{L_m}{L_r} \bar{\psi}_r + L'_s \bar{I}_s \quad (6)$$

Where $L'_s = L_s L_r - L_m^2$. The corresponding expression of \bar{I}_s is

$$\bar{I}_s = \frac{1}{L'_s} \bar{\psi}_s - \frac{L_m}{L_r L'_s} \bar{\psi}_r \quad (7)$$

Substituting equation (7) in (3) and simplifying yields

$$\bar{T}_e = \frac{3}{2} \left(\frac{P}{2} \right) \frac{L_m}{L_r L'_s} \bar{\psi}_r \times \bar{\psi}_s \quad (8)$$

that is, the magnitude of torque is

$$T_e = \frac{3}{2} \left(\frac{P}{2} \right) \frac{L_m}{L_r L'_s} |\psi_r| |\psi_s| \sin \gamma \quad (9)$$

Where γ is the angle between the fluxes. Figure (5) shows the phasor (or vector) diagram for the equation

(8), indicating the vectors $\bar{\psi}_s$, $\bar{\psi}_r$ and \bar{I}_s for positive developed torque. If the rotor flux remains constant and the stator flux is changed incrementally by stator voltage \bar{V}_s as shown, and the corresponding change of γ angle is $\Delta\gamma$, the incremental torque ΔT_e expression is given as

$$\Delta T_e = \frac{3}{2} \left(\frac{P}{2} \right) \frac{L_m}{L_r L'_s} |\psi_r| |\psi_s + \Delta\psi_s| \sin \Delta\gamma \quad (10)$$

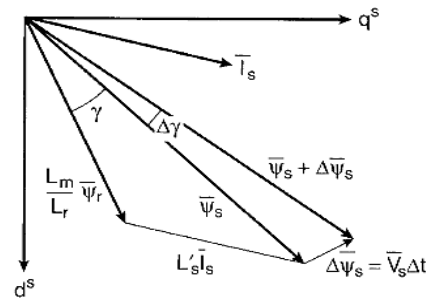


Figure 5 : Stator Flux, Rotor Flux and Stator Current Vectors on ds –qs Plane (Stator Resistance Neglected)

3. Control strategy of DTC

An advanced scalar control technique based on direct torque and flux control (known as DTFC or DTC) was introduced in 1985. The strategy of DTC control is shown in this figure, and its control principle will be explained in the next two figures.

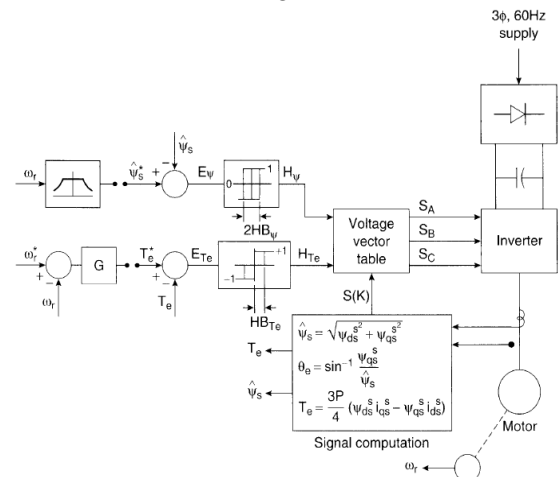


Figure 6 : Direct Torque and Flux Control (DTC)

Basically, it uses torque and stator flux control loops, where the feedback signals are estimated from the machine terminal voltages and currents. The torque command can be generated by the speed loop as shown. The loop errors are processed through hysteresis bands and fed to a voltage vector look-up table. The flux loop has outputs +1 and -1, whereas the torque loop has three

outputs, +1, 0, and -1 as shown. The inverter voltage vector table also gets the information about the location of the stator flux vector $\bar{\psi}_s$ (Figure 7&8). From the three inputs, the voltage vector table selects an appropriate voltage vector to control the PWM inverter switches. The control strategy is based on the torque equation,

$$T_e = \frac{3}{2} \left(\frac{P}{2} \right) \frac{L_m}{L_r L_s} |\psi_r| |\psi_s| \sin \gamma \quad (11)$$

where $\bar{\psi}_s$ and $\bar{\psi}_r$ are the stator and rotor fluxes, respectively, and γ is the angle between them. Note that the control does not use any PWM algorithm or any feedback current signal. It can be used for wide speed ranges including the field-weakening region but excludes the region close to zero speed. DTC control has been used widely, for example, in pump and compressor drives as improvement of open-loop volts/Hz control.

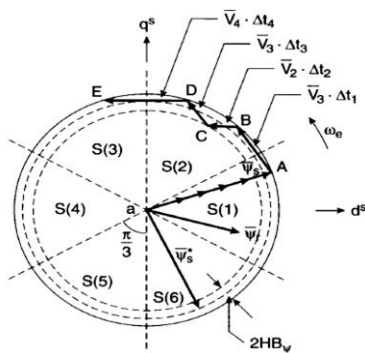


Figure 7 : Stator Flux Vector Trajectory in DTC Control

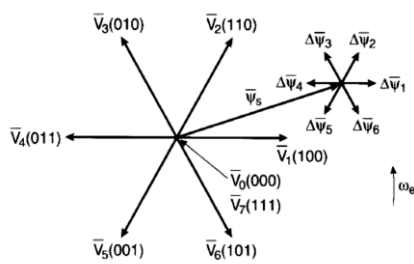


Figure 8: Control of Voltage Vectors to Control Flux Trajectory

The stator flux vector $\bar{\psi}_s$ rotates in a circular orbit within a hysteresis band covering the six sectors as shown in figure (8). The six active voltage vectors and the two zero vectors of the inverter controlled by the look-up table are shown in the table (4). If a voltage vector is applied to the inverter for time Δt , the corresponding flux change is given by the relation $\Delta \bar{\psi}_s = \bar{V}_s \cdot \Delta t$. The

flux increment vector for each voltage vector is indicated in fig (4).

The flux is initially established at zero frequency in the radial trajectory OA. With the rated flux, command torque is applied and the flux vector starts rotating in the counterclockwise direction within the hysteresis band depending on the selected voltage vector. The flux is altered in the radial direction due to flux loop error, whereas the torque is altered by tangential movement of the flux vector. Note that $\bar{\psi}_s$ moves in a jerky manner at γ angle ahead (for $+T_e$) of rotor flux $\bar{\psi}_r$, which has smooth rotation. The jerky variation of stator flux and γ angle introduces the torque ripple. Note that the lowest speed is restricted because of the difficulty of voltage model flux estimation at low frequency.

H_ψ	H_{T_e}	S(1)	S(2)	S(3)	S(4)	S(5)	S(6)
1	1	V_2	V_3	V_4	V_5	V_6	V_1
	0	V_0	V_7	V_0	V_7	V_0	V_7
	-1	V_6	V_1	V_2	V_3	V_4	V_5
-1	1	V_3	V_4	V_5	V_6	V_1	V_2
	0	V_7	V_0	V_7	V_0	V_7	V_0
	-1	V_5	V_6	V_1	V_2	V_3	V_4

Table 4: Switching Table of Voltage Vectors

Voltage vector	V_1	V_2	V_3	V_4	V_5	V_6	V_0 or V_7
ψ_s	↑	↑	↓	↓	↓	↑	0
T_e	↓	↑	↑	↑	↓	↓	↓

Table 5: Flux and Torque Sensitivity by Voltage Vectors.

The voltage vector look-up table for DTC control is shown in Table: 4 for the three inputs [H_ψ , H_{T_e} , and $S(K)$]. The flux trajectory segments AB, BC, CD, and DE by the respective voltage vectors V_3 , V_4 , V_3 , and V_4 are shown in Figure (8). For example, if $H_\psi = -1$, $H_{T_e} = 1$, and $S(K) = S(2)$, vector V_4 will be selected to describe the BC trajectory because at point B, the flux is too high and torque is too low. At point C, $H_\psi = +1$ and $H_{T_e} = +1$, and this will generate V_3 vector from the table. The lower table summarizes the flux and torque sensitivity and direction for applying a voltage vector for the flux location shown in table (5). The flux can be increased by

V_1 , V_2 , and V_6 , whereas it can be decreased by V_3 , V_4 , and V_5 . The zero vectors short circuits the machine terminal and keeps the flux and torque essentially unchanged.

The figure summarizes the essential features of DTC control. Basically, the control is accomplished by simple but advanced scalar control of torque and stator flux by hysteresis-band feedback loops. There is no feedback current control although current sensors are essential for protection. Note that no traditional SPWM or SVM technique is used as in other drives. The indirect PWM control is due to voltage vector selection from the look-up table to constrain the flux within the hysteresis band. Similar to hysteresis band (HB) current control, there will be ripple in current, flux, and torque. The current ripple will give additional harmonic loss, and torque ripple will try to induce speed ripple in a low inertia system. In recent years, the simple HB-based DTC control has been modified by fuzzy and neuro-fuzzy control in inner loops with SVM control of the inverter. Multiple inverter vector selection in SVM within a sample time smoothes current, flux, and torque. However, with the added complexity, the simplicity of DTC control is lost. DTC control can be applied to PM synchronous motor drives also.

III. RESULTS AND DISCUSSION

Simulation

The inputs given to the main circuit shown in figure (5.5) are the supply voltage of 460V, 50 Hz frequency. The speed reference is given as 1000 rpm and load torque is 400 NM.

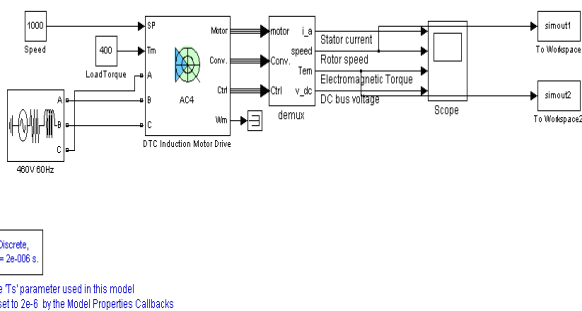


Figure 9: DTC Induction Motor 200HP Drive Circuit

Novel SVPWM Circuit :

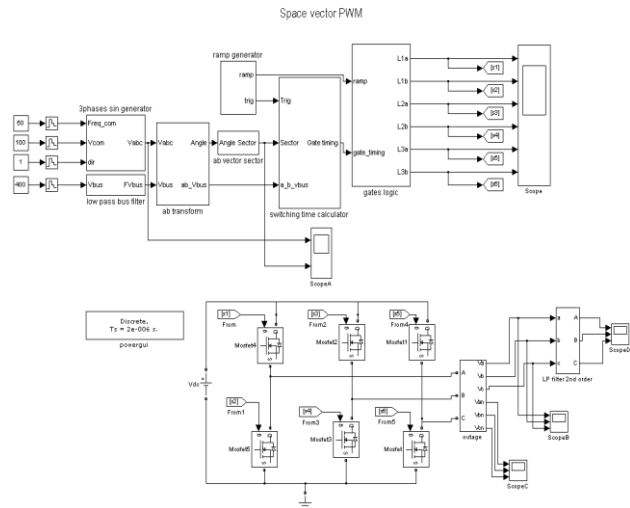


Figure 10 : Novel Space Vector Pulse Width Modulation using in VSI Circuit

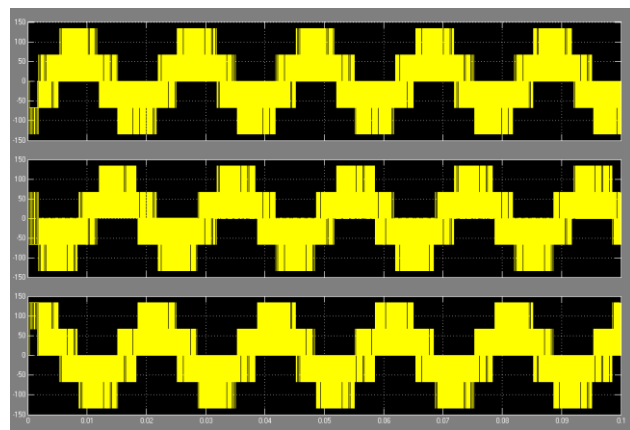


Figure 11: Output waveforms of Inverter

In the main circuit, the nominal rating of the motor is 200HP, 460V, 50HZ. The stator resistance is 14.85mΩ, the initial machine flux value is 0.8 wb, and the maximum switching frequency is 5KHZ.

The respective output waveforms of Direct torque control of Induction motor using novel SVPWM technique are as follows.

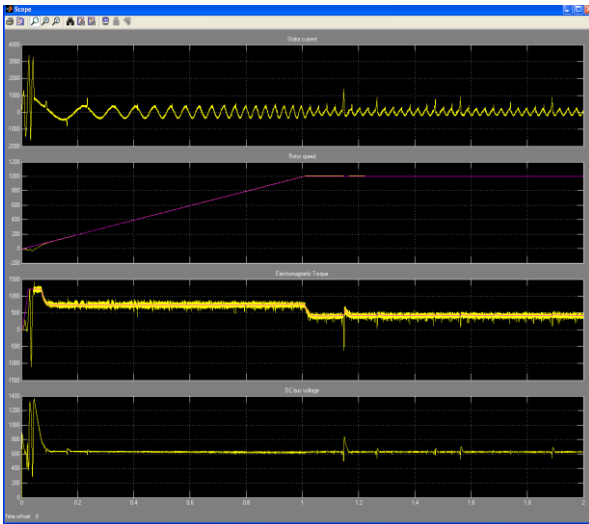


Figure 11 : Various results on DTC using eight sectors with speed reference-1000RPM, load torque-400NM

IV. CONCLUSION

In this paper, a new space vector pulse width modulation technique has been proposed in which a three level voltage source inverter is employed in driving an induction motor using the DTC technique.

A switching table with eight numbers of sectors, which allows direct torque control of the voltage source inverter on the basis of the motor control requirements, has been defined. SVPWM with eight voltage sector, gradually reduces switching frequency in inverter is used in this module. The switching losses are also less when compared with model using six sectors. Performance of torque and speed is not varied with six sector module. The proposed scheme has been tested with low and high speed ranges, performing simulation. The current and torque waveforms emphasize the effectiveness of the control scheme.

V. REFERENCES

- [1] Xavier del Toro Garcia, Antoni Arias, Marcel G. Jayne, and Phil A. Witting “Direct Torque Control of Induction Motors Utilizing Three-Level Voltage Source Inverters”, IEEE TRANSACTIONS ON INDUSTRIAL ELECTRONICS, VOL. 55, NO. 2, FEBRUARY 2008.
- [2] Domenico Casadei, Giovanni Serra “The Use of Matrix Converters in Direct Torque Control of

Induction Machines”, IEEE TRANSACTIONS ON INDUSTRIAL ELECTRONICS, VOL. 48, NO. 6, DECEMBER 2001.

- [3] Romeo Ortega, Nikita Barabanov, and Gerardo Escobar Valderrama, “Torque Control of Induction Motors: Stability Analysis and Performance Improvement”, IEEE TRANSACTIONS ON AUTOMATIC CONTROL, VOL. 46, NO. 8, AUGUST 2001.
- [4] Bose, B. K., Modern Power Electronics and AC Drives, Prentice-Hall, N.J., 2002, Grelet, G. and G. Clerc, Actionneurs électriques, Éditions Eyrolles, Paris, 1997, Krause, P. C., Analysis of Electric Machinery, McGraw-Hill, 1986.
- [5] J. Rodriguez, J. Lai, and F. Z. Peng, “Multilevel inverters: A survey of topologies, controls, and applications,” IEEE Trans. Ind. Electron., vol. 49, no. 4, pp. 724–738, Aug. 2002.
- [6] A. Nabae, I. Takahashi, and H. Akagi, “A new neutral-point-clamped PWM inverter,” IEEE Trans. Ind. Appl., vol. IA-17, no. 5, pp. 518–523, Sep./Oct. 1981.